SIAM J. Appl. Math.
Vol. 74, No. 2, pp. 366–391

HIGHER-ORDER AVERAGING OF FOKKER–PLANCK EQUATIONS FOR NONLINEAR FIBER LAY-DOWN PROCESSES*

L. L. BONILLA†, A. KLAR‡, AND S. MARTIN§

Abstract. We investigate stochastic models for the lay-down of flexible fibers on a moving conveyor belt for the case of small stochasticity and small belt velocity. Using a suitable scaling we obtain a singularly perturbed problem for a stochastic Hamiltonian system and the corresponding Fokker–Planck equation. These equations are investigated using averaging methods. In the present case the impact of the deterministic forcing, i.e., the belt velocity is not captured by the stochastic averaging theorem. To overcome this problem, a formal energy projection method previously introduced by the authors is used, which allows the computation of higher-order stochastic averages for the present highly nonlinear system. The resulting second-order coefficients are computed numerically and a suitably precise scheme is developed. Finally, we illustrate the results of our method with several examples.

Key words. Fokker–Planck equations, stochastic Hamiltonian systems, fiber dynamics, higher-order averaging

AMS subject classifications. 37H10, 60H30, 70H05

DOI. 10.1137/130905332

1. Introduction.

The production of nonwovens in the hygiene, medical, and filter industries is a lay-down process of multiple endless synthetic fibers on a moving conveyor belt. Several hundred or thousand fibers are pressed out of nozzles simultaneously. Turbulent air flows, which also cool down the fiber material, spin the single fiber. The simulation of the spinning process is of great importance for quality improvements, design of new machines, and optimization of production processes. The need for advanced models for the fiber-spinning process has increasingly stimulated mathematical research in recent years; see, e.g., [13, 18]. Simulation tools are currently able to simulate the dynamics of elastic fibers under the influence of three main forces: aerodynamic turbulence, friction with machine parts, and contact with other fibers. The geometries of machines and conveyor belts can be fully integrated. This comes together with a high computational effort. In order to realize complex optimization processes, a faster, approximative simulation is needed. A simplified modeling approach has been developed in [9] and investigated further in [4]. An extension to three-dimensional spinning processes has been presented in [14, 15]. The stochastic parameters of the simplified model are to be calibrated using a detailed simulation. The simplified model considers the lay-down process of a single endless fiber, whose motion is composed of a deterministic pendulum motion around the centre of the spin-

*Received by the editors January 9, 2013; accepted for publication (in revised form) January 6, 2014; published electronically March 20, 2014. This work has been supported by Deutsche Forschungsgemeinschaft (DFG), WE 2003/3-1, KL 1105/18-1, and by Bundesministerium für Bildung und Forschung (BMBF), Verbundprojekt ProFil, 03MS606. Moreover, the work has been supported by the Spanish Ministry of Economy and Competitiveness under grant FIS2011-28838-C02-01.
http://www.siam.org/journals/siap/74-2/90533.html

†Instituto Gregorio Millán, Escuela Politécnica Superior, Universidad Carlos III de Madrid, Avda. de la Universidad 30, Leganés 28911, Spain (bonilla@ing.uc3m.es).

‡Technische Universität Kaiserslautern, Department of Mathematics, Erwin-Schrödinger-Straße, 67663 Kaiserslautern, Germany and Fraunhofer ITWM, Fraunhoferplatz 1, 67663 Kaiserslautern, Germany (klar@mathematik.uni-kl.de).

§Corresponding author. Imperial College London, Department of Mathematics, SW7 2AZ London, UK (stephan.martin@imperial.ac.uk).

ning nozzle and a stochastic noise acting on one variable of the deterministic motion. For the case of a nonmoving conveyor belt, the model has been studied extensively: The model equations can be rewritten as a Hamiltonian system under friction and stochastic noise, governed by a Hamiltonian energy variable. A limit equation for the energy can be derived for the small noise case using the stochastic averaging theorem. A moving conveyor belt enters the model as a small, periodic, and deterministic forcing term whose periodicity is different than the governing Hamiltonian. However, the influence of this forcing term on the energy limit process is not captured by the beforementioned averaging procedure.

In [5], the authors presented a framework of higher-order averaging for such Hamiltonian systems under small stochastic noise and periodic forcing along the lines of averaging procedures presented in [11, 12]. Based on a formal asymptotic expansion of the associated Fokker–Planck equation, the method was developed in general and then applied to standard linear and nonlinear oscillators. Due to the numerical approximations required during the high-order averaging procedure, which will also be discussed below, the applicability of the framework to highly nonlinear systems such as the fiber models has not yet been investigated. The model introduced in [9] is difficult to analyze in its Hamiltonian coordinates, as the transformation induces an instability of the equilibrium distribution even in the absence of conveyor belt motion. In the present paper we find a general description of the noise and forcing terms including conveyor belt motion with stable equilibrium distributions, that approach smoothly the equilibrium distribution at zero conveyor belt motion in Hamiltonian coordinates.

The goal of the present paper is twofold: First we introduce a new fiber model with desirable properties in the Hamiltonian coordinates introduced in [9] that behaves as described before. In this model, the coiling of the polymer fiber is strongly coupled to the spinning movement of the nozzles and it has a stable equilibrium distribution function for the stationary conveyor belt. This allows development of a more complete study for this model than for the original model. Second, we extend the higher-order averaging procedure to the new model with a moving conveyor belt in order to investigate the influence of the belt velocity on the limiting energy equation. The approach is based on a splitting ansatz projecting the probability density f on an energy dependent density Pf and the derivation of a system of equations for both Pf and its remainder Qf. The key idea is then to solve for an approximate solution of Qf to obtain higher-order approximations of Pf. Due to the highly nonlinear Hamiltonian we are dealing with significantly more complicated terms than the oscillator models discussed in [5]. It will turn out again that the first-order approximation for the case of a moving belt yields the same equation for the energy as the nonmoving belt case; and that only the second-order procedure finally leads to the desired accurate asymptotic approximation. In contrast to [5], no explicit formulas can be found for the averaged coefficients, which hence have to be computed numerically. Given the nonlinearity of the problem, these computations require a careful investigation.

The paper is organized as follows: In section 2, we present the original fiber model and its suitable modified version which we investigate henceforth. The standard method of stochastic averaging to zeroth order is revisited in section 3, where effects of small forcing terms are not captured. In section 4 the formal projection procedure for higher-order averaging based on the Fokker–Planck equation from [5] is presented and applied to the present model with computations of the first- and second-order coefficients. Finally, the numerical methods are described and numerical results are presented in section 5.

2. The model. Consider a slender, elastic, nonextensible and endless fiber in a lay-down regime. Let the fiber be produced with the spinning speed v_{spin}, excited into motion by a surrounding highly turbulent air flow, and laid down on a conveyor belt moving with the velocity v_{belt}. Due to its slenderness, the fiber laid on the two-dimensional transport belt is described as a curve $\eta:\mathbb{R}_0^+\to\mathbb{R}^2$. Choosing arc-length parameterization, the nonextensibility condition $\|d\eta/dt\|=1$ holds by setting

$$d\eta=(\cos\alpha,\sin\alpha)\,dt,$$

where α denotes the angle of the fiber relative to the direction of motion e_1 of the transport belt. The reference point of the spinning process determined by the position of the nozzle moves in the coordinate system of the transport belt in the direction $-e_1$. Thus,

$$\xi(t)=\eta(t)-(-\kappa te_1)=\eta(t)+\kappa te_1$$

describes the deviation of the fiber from the reference point as a function of the arc-length parameter t, where $\kappa=v_{belt}/v_{spin}\in[0,1]$ is the ratio between the belt and spinning speeds. Generalizing the approach in [4], we model (ξ,α) by the stochastic differential system

$$\mathrm{d}\xi_1=(\cos\alpha+\kappa)\mathrm{d}t, \tag{2.1a}$$

$$\mathrm{d}\xi_2=\sin\alpha\mathrm{d}t, \tag{2.1b}$$

$$\mathrm{d}\alpha=F(\xi,\alpha)\mathrm{d}t+G(\xi,\alpha)\mathrm{d}W_t. \tag{2.1c}$$

Here, the change of the angle α is characterized by the deterministic buckling/coiling F of the fiber and by the random fluctuations $G\mathrm{d}W_t$ due to the interaction of the fiber with the external turbulent air flow. Here, W_t denotes a one-dimensional Wiener process.

The model investigated, for example, in [9] is given by $F=-\nabla V(\xi)\cdot\tau^{\perp}$ with $\tau(\alpha)^{\perp}=(-\sin(\alpha),\cos(\alpha))^T$, $V:\mathbb{R}^2\to\mathbb{R}$, and $G=A=\text{const}$. The parameter A and the potential V depend on the specific application and need to be adapted to experimental data. The general deterministic coiling behavior of flexible fibers has been studied for example in [17]. The function V in the model prescribes its amplitude that depends on the lay-down process. We restrict ourselves to isotropic processes, i.e., we consider $V(\xi)=B(\|\xi\|)$. In this case $\nabla V(\xi)=B'(\|\xi\|)\frac{\xi}{\|\xi\|}=b(\|\xi\|)\frac{\xi}{\|\xi\|}$.

Introducing polar coordinates $\xi=(r\cos\phi,r\sin\phi)^T$, $r=\|\xi\|$ and the angle $\beta=\alpha-\phi$ with ϕ in ξ-space, as illustrated in [9, Figure 1], the given stochastic differential system can be rewritten in terms of $(r,\beta)\in[0,\infty)\times[0,2\pi]$ as

$$\mathrm{d}r_t=\cos\beta_t\,\mathrm{d}t+\kappa\cos\phi_t\mathrm{d}t, \tag{2.2a}$$

$$\mathrm{d}\beta_t=\left(F-\frac{1}{r_t}\sin\beta_t\right)\mathrm{d}t+\kappa\frac{\sin\phi_t}{r_t}\mathrm{d}t+G\,\mathrm{d}W_t, \tag{2.2b}$$

$$\mathrm{d}\phi_t=\frac{\sin\beta_t-\kappa\sin\phi_t}{r_t}\mathrm{d}t. \tag{2.2c}$$

We note that for the above example we have $F=b(r)\sin\beta$. Here, we consider functions $F=b(r)\sin\beta+\kappa f_1(r,\phi,\beta)+A^2f_2(r,\phi,\beta)$ and $G=Ag(r,\phi,\beta)$. That means, we restrict ourselves to systems with $F=b(r)\sin\beta$ for A and κ equal to 0. In this case, the unperturbed deterministic (r,β)-system with $A=0$ and $\kappa=0$ moves on closed orbits

in the (r,β)-plane with fixed points $(r,\beta)=(1,\pi/2)$ for $\beta\in[0,\pi)$ and $(r,\beta)=(1,3\pi/2)$ for $\beta\in(\pi,2\pi]$. The periodic orbits are given by the level sets $H(r,\beta)=h\in[0,\infty)$ of the Hamiltonian

$$H(r,\beta)=B(r)-\ln r-\ln\sin\beta. \tag{2.3}$$

We normalize $B(1)=0, B'(1)=1$. The associated Fokker–Planck equation (see [20]) is

$$\partial_t f+\partial_r((\cos\beta+\kappa\cos\phi)f)+\partial_\beta\left(\left(F-\frac{\sin\beta}{r}+\kappa\frac{\sin\phi}{r}\right)f\right)=\frac{1}{2}\partial_\beta^2(G^2 f). \tag{2.4}$$

One may rewrite the system in Hamiltonian coordinates under the transformation $z=\ln\tan(\beta/2)$, for which $z'(\beta)=\frac{1}{\sin\beta}$, $\beta(z)=2\arctan(\exp z)$, and $\beta'(z)=\sin(\beta)$ hold. This leads to

$$\mathrm{d}r=-\frac{\partial}{\partial z}H(r,z)\mathrm{d}t+\kappa\cos\phi\mathrm{d}t, \tag{2.5a}$$

$$\begin{aligned}\mathrm{d}z=&\frac{\partial}{\partial r}H(r,z)\mathrm{d}t+\frac{\kappa}{\sin\beta(z)}\left(\frac{\sin\phi}{r}+f_1\right)\mathrm{d}t\\&+\frac{A^2}{\sin\beta(z)}\left(f_2-\frac{g^2\cos\beta(z)}{2\sin\beta(z)}\right)\mathrm{d}t+\frac{Ag}{\sin\beta(z)}\mathrm{d}W_t,\end{aligned} \tag{2.5b}$$

$$\mathrm{d}\phi=\frac{\sin\beta(z)}{r}\mathrm{d}t-\frac{\kappa}{r}\sin\phi\mathrm{d}t \tag{2.5c}$$

with

$$\partial_r H(r,z)=b(r)-\frac{1}{r}\ ,\ \partial_z H(r,z)=-\cos(\beta(z)). \tag{2.6}$$

The closed deterministic orbits in the (r,z)-plane are shown in Figure 7. The associated Fokker–Planck equation for the density of the process reads

$$\begin{aligned}\partial_t\rho+\partial_r[(\kappa\cos\phi-H_z)\rho]+\partial_z\left[\left(H_r+\frac{\kappa}{\sin\beta}\left(\frac{\sin\phi}{r}+f_1\right)+\frac{A^2}{\sin\beta}\left(f_2-\frac{g^2\cos\beta}{2\sin\beta}\right)\right)\rho\right]\\+\partial_\phi\left[\frac{\sin\beta-\kappa\sin\phi}{r}\rho\right]=\frac{A^2}{2}\partial_z^2\left(\frac{g^2\rho}{\sin^2\beta}\right).\end{aligned} \tag{2.7}$$

If $g\partial_\beta g=f_2$, which we assume from now on, then the stationary solution of the equation with $\kappa=0$ is, in (r,z)-coordinates, given by

$$\rho_S(r,z)=\exp(-H(r,z)). \tag{2.8}$$

The relation $g\partial_\beta g=f_2$ ensuring that the exponential distribution (2.8) is a stable equilibrium solution for $\kappa=0$ plays a role similar to the fluctuation-dissipation relation that ensures that the Fokker–Planck equation describing Brownian motion has a Boltzmann equilibrium (see [22]). As the parameter A balances noise and part of the separated friction terms, A controls the rate of convergence towards the unperturbed equilibrium ρ_S, but does not influence its shape.

Remark 2.1. Linearizing the unperturbed system in (2.5) around the fixed point $(r,z)=(1,0)$ we obtain a harmonic oscillator

$$\mathrm{d}r_t=\beta_t\,\mathrm{d}t, \tag{2.9a}$$

$$\mathrm{d}\beta_t=(b'(1)+1)(r_t-1)\mathrm{d}t, \tag{2.9b}$$

$$\mathrm{d}\phi_t=(1-(r_t-1))\mathrm{d}t, \tag{2.9c}$$

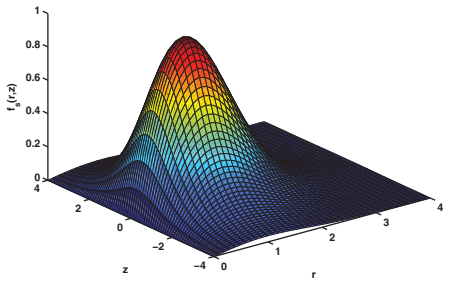

FIG. 1. *The formal equilibrium* (2.13) *of* (2.12) *in* (r,z)*-space.*

with the Hamiltonian function

$$H_{lin}(r,z)=\frac{1}{2}\Big(b'(1)+1\Big)(r-1)^2+\frac{1}{2}z^2.$$

Its period of motion is $T_{lin}=2\pi/\sqrt{b'(1)+1}$. For small h, the nonlinear period T_h of motion tends to the linearized one. For a discussion of higher-order averaging procedures for standard oscillators we refer again to [5].

In the following we include a short discussion of different possibilities for choosing f_1 and g. The simplest choice is, as in the original model, to choose $f_1=0$ and $g=1$. In the absence of deterministic friction, $\kappa=0$, the associated Fokker–Planck equation in (r,β) reads

$$\partial_t f+\partial_r(\cos\beta f)+\partial_\beta\left((b(r)-1/r)\sin\beta f\right)=\frac{A^2}{2}\partial_\beta^2 f. \tag{2.10}$$

The stationary solution on the torus $\beta\in[0,2\pi)$ is

$$f_s(r,\beta)=e^{-B(r)}r. \tag{2.11}$$

Exponential convergence towards this stable equilibrium can be proven; see [7]. In Hamiltonian form the Fokker–Planck equation (FPE) in the absence of friction ($\kappa=0$) reads

$$\partial_t f+\partial_r(-H_z f)+\partial_z\left(\left(H_r-\frac{A^2}{2}\frac{\cos\beta(z)}{\sin^2\beta(z)}\right)f\right)=\frac{A^2}{2}\partial_z^2\left(\frac{1}{\sin\beta(z)}f\right). \tag{2.12}$$

The formal equilibrium of (2.12) is

$$f_s(r,z)=\exp(-H(r,z))=e^{-B(r)}r\sin\beta(z), \tag{2.13}$$

which fits (2.11) since $\beta'(z)=\sin(\beta(z))$. In Figure 1 (2.13) is plotted in (r,z)-space. In these coordinates however, (2.13) is not a well-posed stable equilibrium of (2.12). This is due to the fact that both drift and diffusion coefficients depending on $A^2/2$ in (2.12) diverge at infinity. As we illustrate in Figure 2, the drift term is a point symmetric function with positive derivative at zero that tends to infinity for $z\to+\infty$. Since all other terms are bounded for any fixed r, there is a self-increasing drift towards $z\to\pm\infty$. The diffusion coefficient is an axially symmetric function diverging at infinity. The reason behind the instability of (2.13) is the fact, that the transformation $z:\beta\mapsto z$ is only defined for the restricted domain $\beta\in[0,\pi)$ and maps from $\beta\in[0,\pi)$ into $\mathbb{R}$ and not from the full torus $\beta\in[0,2\pi)$. This is important, since the mechanism leading to

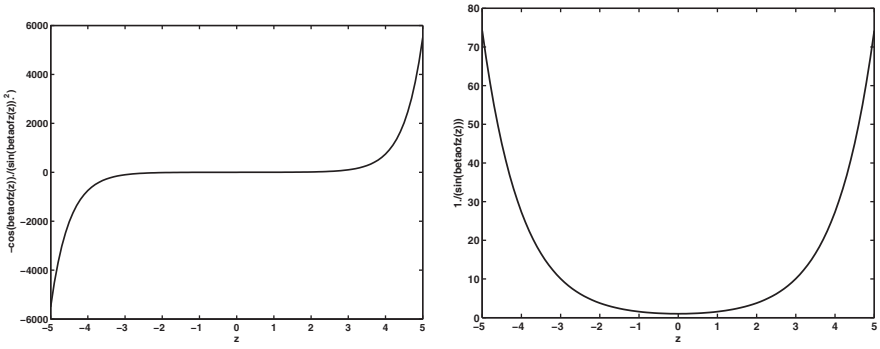

(a) drift component $-\frac{\cos\beta(z)}{\sin^2\beta(z)}$ (b) diffusion coefficient $\frac{1}{\sin\beta(z)}$

FIG. 2. *Illustration of drift and diffusion terms appearing in the FPE* (2.12) *plotted against varying* z. *For highly positive (negative) values of* z, *the drift value is increasingly negative (positive). Hence, drift always acts against the equilibrium point* $(r,z)=(1,0)$. *Together with diverging diffusion at infinity, the formal equilibrium* (2.13) *shown in Figure* 1 *is an unstable stationary solution.*

the uniform equilibrium (2.11) in (2.2) is a homogenization over the full torus; see [7] for a rigorous proof of convergence to equilibrium. It is not given as a balance of forces in system (2.5) defined on $r\in\mathbb{R}^+,\beta\in[0,\pi)$ as in the oscillator models in [5]. In this case, although the zeroth-order averaging method works fine, we are not able to apply the method of higher-order stochastic averaging successfully. We also note that no further transformation to different Hamiltonian coordinates for (2.2) that keep $\beta\in[0,2\pi)$ are known.

The above observations are, however, not true for all choices of f_1 and g. In the following, we choose to set $f_1=\frac{\sin\phi}{r}(\sin\beta-1)$, $g=\sin\beta$ and hence obtain more regular coefficients in the (r,z) equations

$$\mathrm{d}r_t=-\frac{\partial}{\partial z}H(r,z)\mathrm{d}t+\kappa\cos\phi_t\mathrm{d}t, \tag{2.14a}$$

$$\mathrm{d}z_t=\frac{\partial}{\partial r}H(r,z)\mathrm{d}t+\left(\frac{\kappa\sin\phi_t}{r_t}+\frac{A^2}{2}\cos\beta(z_t)\right)\mathrm{d}t+A\mathrm{d}W_t, \tag{2.14b}$$

$$\mathrm{d}\phi_t=\frac{\sin\beta(z_t)}{r_t}\mathrm{d}t-\frac{\kappa}{r_t}\sin\phi_t\mathrm{d}t. \tag{2.14c}$$

The Hamiltonian motion is unchanged, as well as the unforced equilibrium ($\kappa=0$), which reads $f_s(r,z)=\exp(-H(r,z))$. However, in this case the new diffusion and drift terms allow for a stable equilibrium. The associated Fokker–Planck equation is

$$\partial_t f+\partial_r[(\kappa\cos\phi-H_z)f]+\partial_z\left[\left(H_r+\frac{A^2}{2}\cos\beta+\frac{\kappa\sin\phi}{r}\right)f\right]+\partial_\phi\left[\frac{\sin\beta-\kappa\sin\phi}{r}f\right]=\frac{A^2}{2}\partial_z^2 f. \tag{2.15}$$

We obtain a new model close to the equations treated in [5] with a meaningful physical interpretation for f_1,g: Restricting the stochastic noise on β such that $\beta\in(0,\pi)$ by setting $g=\sin\beta$ implies $\alpha>\phi$ for all times, thus the tangent to the fiber is left orientated compared to its Cartesian position vector. The choice of f_1 than follows naturally to obtain bounded terms in (2.14b), (2.14c). In this fiber model, the coiling

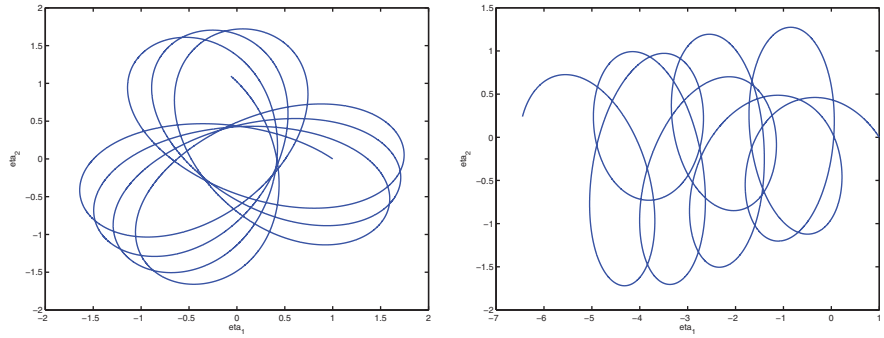

(a) $\kappa = 0, A = 0$ (b) $\kappa = 0.1, A = 0$

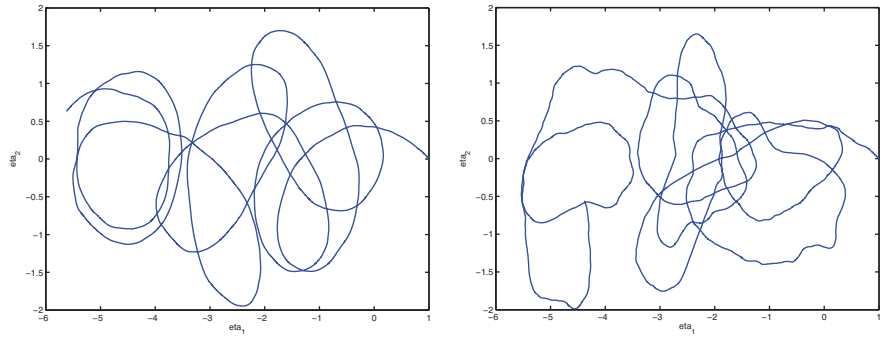

(c) $\kappa = 0.1, A = \sqrt{0.1}$ (d) $\kappa = 0.1, A = 1$

FIG. 3. *Exemplary trajectories for the model* (2.14)*: While the basic Hamiltonian motion* (a) *is identical to previously studied fiber models (see* [9]*), the new forcing and noise terms perturb the fiber in angular coordinates without deviating strongly from the deterministic coiling behavior. For a fixed belt velocity* $\kappa = 0.1$ *and increasing noise parameter A,* (b) *shows a moving belt without noise, while* (c) *and* (d) *show that the fiber wiggles under stochastic influence without losing its rotational direction, since* $\beta \in (0, \pi)$*. Model* (2.14) *thus represents a situation where the initial spinning direction induced by the production process has a strong influence on the resulting fiber, e.g., due to material properties of the polymer. The trajectories are shown in curve coordinates* η *on the conveyor belt. (Monte Carlo simulations with a standard Euler scheme are run on* $T = [0, 50]$ *with step size* $\Delta t = 10^{-4}$ *and initial values* $[r_0, z_0, \phi_0] = [1, 1, 0]$*.)*

behavior given from the deterministic motion has a stronger influence on the fiber lay-down than in previously considered models, where friction and noise led to arbitrary rotations. We illustrate this behavior with some exemplary trajectories for varying noise amplitude in Figure 3. Note that the restriction on β entirely depends on the initial value $\beta_0 = \beta(0)$ and the restriction $\beta \in (\pi, 2\pi)$ would be equally possible using a modified transformation $\tilde{z}$. Applying higher-order stochastic averaging is at first sight, a substantially more subtle problem than the oscillator problems in [5]: There is a highly nonlinear Hamiltonian, a secondary frequency that is not constant but coupled to the evolution of the system (see (2.14c)), and deterministic friction applies not to one but to all three equations of (2.14). Nevertheless, in the next section, we show that the techniques from [5] can be applied to the modified fiber model (2.14), if the numerical evaluation of the averaged coefficients is done more carefully.

3. Stochastic averaging theorem. In the following we consider the lay-down processes (2.14) with small noise $A = \sqrt{\epsilon}\tilde{A}$ and small velocity $\kappa = \epsilon\tilde{\kappa}$ on associated

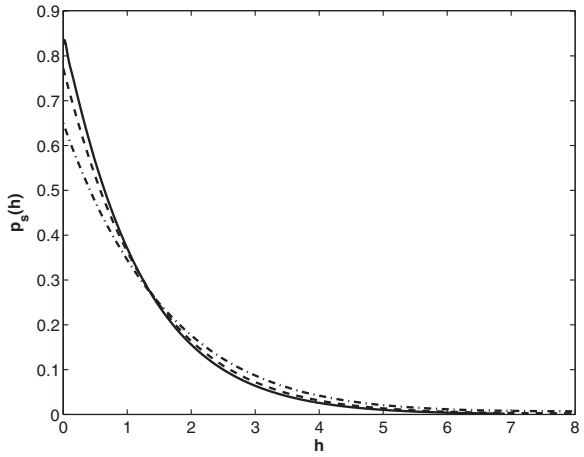

FIG. 4. *Simulated stationary distribution of H_t^ϵ for increasing values of belt velocity: $\kappa=0$ (solid), $\kappa=0.1$ $(--)$, $\kappa=0.2$ $(-\cdot)$. There is a substantial deviation of the unperturbed equilibrium $\kappa=0$, which is not captured by the stochastic averaging theorem.*

long "time" scales $t=\tilde{t}/\epsilon$ with $0<\epsilon\ll 1$. In this case, a simplified approximation of the energy dynamics can be given by stochastic averaging. This leads to a reduced system as $\epsilon\to 0$, i.e., a stochastic differential equation for the limit energy process for which we determine the drift and variance coefficients. Dropping the tildes, the rescaled $(r_t^\epsilon, z_t^\epsilon)$-system reads

$$\mathrm{d}r_t^\epsilon = \frac{1}{\epsilon}\cos\beta_t^\epsilon\,\mathrm{d}t + \kappa\cos\phi_t^\epsilon\mathrm{d}t, \tag{3.1a}$$

$$\mathrm{d}z_t^\epsilon = \frac{1}{\epsilon}\left(b(r_t^\epsilon)-\frac{1}{r_t^\epsilon}\right)\mathrm{d}t + \kappa\frac{\sin\phi_t^\epsilon}{r_t^\epsilon}\mathrm{d}t + \frac{A^2}{2}\cos\beta_t^\epsilon\mathrm{d}t + A\,\mathrm{d}W_t, \tag{3.1b}$$

$$\mathrm{d}\phi_t^\epsilon = \frac{1}{\epsilon}\frac{\sin\beta_t^\epsilon}{r_t^\epsilon}\mathrm{d}t - \kappa\frac{\sin\phi_t^\epsilon}{r_t^\epsilon}\mathrm{d}t. \tag{3.1c}$$

Applying Ito's formula for the energy process $H_t^\epsilon = H(r_t^\epsilon, z_t^\epsilon)$ we obtain the equation

$$\begin{aligned}\mathrm{d}H_t^\epsilon = {}& \kappa\left(b(r_t)-\frac{1}{r_t}\right)\cos\phi_t\mathrm{d}t - \kappa\cos\beta(z_t)\frac{\sin\phi_t}{r_t}\mathrm{d}t \\ & - \frac{A^2}{2}(\cos^2\beta(z_t^\epsilon)-\sin^2\beta_t^\epsilon)\mathrm{d}t - A\cos\beta_t^\epsilon\mathrm{d}W_t.\end{aligned} \tag{3.2}$$

Figure 4 shows the stationary distributions of the H_t^ϵ-process for increasing values of κ together with the explicit solution for the nonmoving belt case. The stationary distributions are computed with a Monte-Carlo simulation of the full system (2.14c) or, equivalently, (3.1) with $\epsilon=1$. The energy process is evaluated for $M=1000000$ trajectories simulated on the time grid $T=[0,500], \Delta t=0.001$ and initial conditions $f_0(x,v,\phi)\sim\delta_{rz}(r=1,z=0)\cdot\mathcal{U}_\phi([0,2\pi])$. We can see, that the stationary distribution is influenced by κ, and that larger values of H gain dominance with increasing belt velocity. We remark, that the standard variance error of the simulation is too small to be shown in Figure 4 and much smaller than the κ-induced deviations.

Using formally the stochastic averaging theorem (see, e.g., [10] or [19] and [1, 2] for an application to stochastic Hamiltonian systems), the limit process for H_t^ϵ as ϵ

tends to 0 is given by H_t^0 with

$$\mathrm{d}H_t^0 = a(H_t^0)\mathrm{d}t + \sigma(H_t^0)\,\mathrm{d}W_t. \tag{3.3}$$

Here drift and variance are

$$a(h) = \frac{A^2}{2}(\overline{\sin^2\beta(z)} - \overline{\cos^2\beta(z)}) + \kappa\overline{\left(b(r) - \frac{1}{r}\right)\cos\phi - \cos\beta(z)\frac{\sin\phi}{r}}, \tag{3.4a}$$

$$\sigma^2(h) = A^2\overline{\cos^2\beta(z)}. \tag{3.4b}$$

We did use the notation

$$\overline{f} = \overline{f}(h) = \lim_{T\to\infty}\frac{1}{T}\int_0^T f(r_t, z_t, \phi_t)\mathrm{d}t = \lim_{T\to\infty}\int_0^1 f(r_{sT}, z_{sT}, \phi_{sT})\mathrm{d}s \tag{3.5}$$

for the limiting time average of a function over an unperturbed motion (r_t, z_t, ϕ_t) with constant energy $H(r_t, z_t) = h$ and period length T_h. For functions of Hamiltonian periodicity, (3.5) reduces to the time average over one sphere

$$\overline{f}(h) = \frac{1}{T_h}\int_0^{T_h} f(r_t, z_t)\mathrm{d}t. \tag{3.6}$$

The limiting averages in (3.4a), depending on κ, average to zero due to the Riemann–Lebesgue lemma. Therefore, the averaged coefficients for moving and nonmoving belts in (3.3) are identical and given as

$$a(h) = \frac{A^2}{2}(\overline{\sin^2\beta(z)} - \overline{\cos^2\beta(z)}), \tag{3.7a}$$

$$\sigma^2(h) = A^2\overline{\cos^2\beta(z)}. \tag{3.7b}$$

Hence, there is no difference for the energy equation for moving and nonmoving belts at the approximation given by the stochastic averaging theorem. We note that the Fokker–Planck equation associated with (3.3) is

$$\partial_t p + \partial_h(a(h)p) = \frac{1}{2}\partial_h^2(\sigma^2(h)p). \tag{3.8}$$

The equation is complemented with an initial condition and conservation of mass

$$\int_0^\infty p(t,h)\mathrm{d}h = 1.$$

Remark 3.1. The stationary energy distribution of the unperturbed process reads

$$\begin{aligned} p_s(h) &= \frac{\mathrm{d}}{\mathrm{d}h}\int_{H(r,z)<h} f_s(r,z)\,\mathrm{d}r\,\mathrm{d}z = Ce^{-h}\frac{\mathrm{d}}{\mathrm{d}h}\int_{H(r,z)<h}\mathrm{d}r\,\mathrm{d}z \\ &= Ce^{-h}T_h \end{aligned} \tag{3.9}$$

because the period of motion of the deterministic system is given by

$$T_h = \frac{\mathrm{d}}{\mathrm{d}h}\int_{H(r,z)<h}\mathrm{d}r\,\mathrm{d}z. \tag{3.10}$$

The stationary solution of (3.8) with coefficients (3.7) is identical to (3.9), hence no information on the stationary energy distribution is lost in the averaging procedure for $\kappa = 0$.

4. Higher-order averaging of Fokker–Planck equations. In this section, we consider the Fokker–Planck equation (2.15) in order to develop higher-order averaging procedures instead of the system of stochastic differential equations (2.14); see also [11, 12]. We describe an approach based on an energy projection method developed in [5]. This will yield in special cases explicit formulas for the averaged problems; however, in general, the asymptotic theory has to be combined with a numerical approach to compute the limit coefficients. The section is divided as follows: We introduce the projection operators and split the FPE into an equivalent system of two equations in section 4.1. A formal second-order asymptotic expansion is presented in section 4.2. The resulting equations are further approximated choosing a simplifying assumption in section 4.3. The coefficients of the approximated system are then determined explicitly or numerically to various orders and the corresponding higher-order coefficients are presented.

4.1. Resulting set of exact equations. Rescaling the Fokker–Planck equation (2.15) using $A=\sqrt{\epsilon}\tilde{A}$, $t=\tilde{t}/\epsilon$, and $\kappa=\epsilon\tilde{\kappa}$ gives

$$\partial_t f+\partial_r\left[\left(\kappa\cos\phi-\frac{1}{\epsilon}H_z\right)f\right]+\partial_z\left[\left(\frac{1}{\epsilon}H_r+\frac{A^2}{2}\cos\beta+\frac{\kappa}{r}\sin\phi\right)f\right] + \partial_\phi\left[\frac{\sin\beta}{\epsilon r}-\frac{\kappa\sin\phi}{r}f\right]=\frac{A^2}{2}\partial_z^2 f\,. \tag{4.1}$$

Following [12] and defining

$$\begin{aligned}\mathcal{L}_2 f&=\partial_r(H_z f)-\partial_z(H_r f)-\partial_\phi\left(\frac{\sin\beta}{r}f\right),\\ \mathcal{L}_1 f&=-\kappa\partial_r(\cos\phi f)-\kappa\frac{\sin\phi}{r}\partial_z f+\kappa\partial_\phi\left(\frac{\sin\phi}{r}f\right)-\frac{A^2}{2}\partial_z(\cos\beta f)+\frac{A^2}{2}\partial_z^2 f,\end{aligned} \tag{4.2}$$

(4.1) can be rewritten as

$$\partial_t\rho=\frac{1}{\epsilon}\mathcal{L}_2\rho+\mathcal{L}_1\rho. \tag{4.3}$$

To formulate the higher-order averaging ansatz, let us start with some definitions. We define the *energy average* of functions in phase space (see [22])

$$p(h,t):=\langle f\rangle:=\partial_h\int_{H(r,z)\le h} f(r,z,\phi,t)\mathrm{d}r\mathrm{d}z\mathrm{d}\phi, \tag{4.4}$$

which we formally write as $p(h,t)=\int\delta(H(r,z)-h)f(r,z,\phi,t)\mathrm{d}r\mathrm{d}z\mathrm{d}\phi$. The corresponding *energy projection* from functions in phase space onto functions of energy is

$$(Pf)(r,z,t):=\frac{p(H(r,z),t)}{2\pi\Omega(H(r,z))}\,,\ \text{where}\ \Omega(h):=\frac{\langle 1\rangle}{2\pi}=\int\delta(H(r,z)-h)\mathrm{d}r\mathrm{d}z. \tag{4.5}$$

Using the equality of energy average and time average, which is true since the ergodic theorem holds trivially for the periodic deterministic, unforced Hamiltonian system on a sphere of constant energy, we have

$$Pf=\overline{f}=\frac{1}{T_h}\int_0^{T_h} f(r(s),z(s),\phi(s))\mathrm{d}s,\quad \overline{f}=\frac{\langle f\rangle}{2\pi\Omega}. \tag{4.6}$$

The distribution function f is then decomposed into

$$f(r,z,\phi,t) = Pf(r,z,t) + \epsilon Qf(r,z,\phi,t) \quad \text{with} \quad \overline{Qf} = 0, \tag{4.7}$$

where the scaling factor ϵ indicates that the Hamiltonian motion dominates small forcing and small noise terms.

Remark 4.1. We note that $T_h = T(h) = \Omega(h)$, and therefore the stationary solution of the unperturbed case $\kappa = 0$ $p_s(h) = Ce^{-h}T(h)$ fulfills $-\frac{p_s}{\Omega} = \partial_h(\frac{p_s}{\Omega})$ and $-Pf = \partial_h Pf$ (see [3]).

To obtain a differential equation in terms of the energy H, we formally apply the energy average (4.4) on the Fokker–Planck equation (4.1) and insert the splitting (4.7). The result is subtracted from (4.1) to obtain a differential equation for Qf. Since $\langle \mathcal{L}_2 f \rangle = 0$, we get

$$\partial_t p - \langle \mathcal{L}_1 Pf \rangle = \epsilon \langle \mathcal{L}_1 Qf \rangle , \tag{4.8a}$$

$$\epsilon \partial_t Qf = \partial_t f - \partial_t \frac{p}{2\pi\Omega} = \left(\frac{1}{\epsilon}\mathcal{L}_2 + \mathcal{L}_1 \right)(Pf + \epsilon Qf) - \frac{1}{2\pi\Omega}\langle \mathcal{L}_1 (Pf + \epsilon Qf) \rangle . \tag{4.8b}$$

We compute the occurring averages in the following lemma.

LEMMA 4.1.

$$\langle \mathcal{L}_1 Pf \rangle = -\frac{A^2}{2}\partial_h \left(\overline{\sin^2\beta(z) - \cos^2\beta(z)}\, p \right) + \frac{A^2}{2}\partial_h^2 \left(\overline{\cos^2\beta(z)}\, p \right) , \tag{4.9a}$$

$$\begin{aligned} \langle \mathcal{L}_1 Qf \rangle = {} & -\kappa \partial_h \langle H_r \cos\phi Qf \rangle + \kappa \partial_h \left\langle \frac{1}{r}\cos\beta(z)\sin\phi Qf \right\rangle \\ & - \frac{A^2}{2}\partial_h \langle (\sin^2\beta(z) - \cos^2\beta(z)) Qf \rangle + \frac{A^2}{2}\partial_h^2 \langle \cos^2\beta(z) Qf \rangle . \end{aligned} \tag{4.9b}$$

Proof. We start by computing

$$\begin{aligned} \langle \mathcal{L}_1 f \rangle = {} & \int \delta(H(r,z) - h)\mathcal{L}_1 f \, \mathrm{d}r\mathrm{d}z\mathrm{d}\phi \\ = {} & \int \delta(H(r,z) - h) \Bigg[-\kappa \partial_r (\cos\phi f) - \kappa \frac{\sin\phi}{r}\partial_z f + \kappa \partial_\phi \left(\sin\phi \frac{1}{r}\rho \right) \\ & - \frac{A^2}{2}\partial_z (\cos\beta(z) f) + \frac{A^2}{2}\partial_z^2 f \Bigg] \mathrm{d}r\mathrm{d}z\mathrm{d}\phi. \end{aligned} \tag{4.10}$$

Performing integration by parts and using the chain rule gives

$$\begin{aligned} \langle \mathcal{L}_1 f \rangle = {} & -\int \partial_H \delta(H(r,z) - h) \Bigg[-\kappa H_r \cos\phi f - \kappa H_z \frac{\sin\phi}{r} f \\ & - \frac{A^2}{2} H_z (\cos\beta(z) f - \partial_z f) \Bigg] \mathrm{d}r\mathrm{d}z\mathrm{d}\phi. \end{aligned} \tag{4.11}$$

Integrating by parts and using the chain rule again yields

$$\begin{aligned} \langle \mathcal{L}_1 f \rangle = {} & -\int \partial_H \delta(H(r,z) - h) \Bigg[-\kappa H_r \cos\phi f - \kappa H_z \frac{\sin\phi}{r} f \\ & - \frac{A^2}{2} (H_z \cos\beta(z) f + H_{zz} f) \Bigg] \mathrm{d}r\mathrm{d}z\mathrm{d}\phi \\ & + \frac{A^2}{2} \int \partial_H^2 \delta(H(r,z) - h)(H_z)^2 f \, \mathrm{d}r\mathrm{d}z\mathrm{d}\phi. \end{aligned} \tag{4.12}$$

Again, a similar computation yields $\int \delta(H(x,v)-h)\mathcal{L}_2 f \mathrm{d}x\mathrm{d}v\mathrm{d}\phi = 0$. We replace $\partial_H \delta(H(x,v)-h) = -\partial_h \delta(H(x,v)-h)$. Inserting now $f = Pf + \epsilon Qf$ we obtain

(4.13)
$$\langle \mathcal{L}_1 f\rangle = \int \partial_h \delta(H(r,z)-h)\left[-\kappa H_r \cos\phi - \kappa H_z \frac{\sin\phi}{r} - \frac{A^2}{2}\left(H_z \cos\beta(z) + H_{zz}\right)\right] \cdot (Pf+\epsilon Qf)\mathrm{d}r\mathrm{d}z\mathrm{d}\phi + \frac{A^2}{2}\int \partial_h^2 \delta(H(r,z)-h)(H_z)^2 (Pf+\epsilon Qf)\mathrm{d}r\mathrm{d}z\mathrm{d}\phi.$$

For the integrals over Pf, we write Pf outside the integral, since it depends on r, z only through $H(r,z)=h$. The average over $\sin\phi, \cos\phi$ drop out for Pf. Since $H_z = -\cos\beta, H_{zz} = \sin^2\beta$ the remaining expression is

$$\begin{aligned}\langle \mathcal{L}_1 f\rangle = {} & \frac{A^2}{2}\partial_h\left(\overline{\cos^2\beta(z) - \sin^2\beta(z)}p\right) + \frac{A^2}{2}\partial_h^2\left(\overline{\cos^2\beta(z)}p\right) \\ & + \epsilon\partial_h\left[-\kappa\langle H_r\cos\phi Qf\rangle + \kappa\left\langle \cos\beta(z)\frac{\sin\phi}{r}Qf\right\rangle \right. \\ & \left. + \frac{A^2}{2}\left\langle \cos^2\beta(z) - \sin^2\beta(z) Qf\right\rangle\right] + \epsilon\partial_h^2\left\langle \cos^2\beta(z) Qf\right\rangle. \end{aligned} \tag{4.14}$$

□

Inserting the results from Lemma 4.1 in (4.8) and taking $\mathcal{L}_2 Pf = 0$ into account, we obtain a system of exact equations, whose solution is equivalent to a solution of the Fokker–Planck equation (4.1).

4.2. First- and second-order asymptotic analysis. In this section, we carry on with the above ansatz and show formally how to derive approximate equations for the energy process. Here, the general asymptotic procedure is presented and in the next section a simplification is introduced which is used for the explicit calculations. The idea is to express Qf in (4.8a) by an approximate solution of (4.8b). We assume that Qf depends on time only through its dependence on p and use the equation for p in order to calculate $\partial_t Qf$ to the necessary order in ϵ. Once this is substituted in the equation for Qf, we can solve it to the required order and insert back the result in the p-equation. This is exactly the Chapman–Enskog method [6] adapted to this problem. From (4.8) we have the system of exact equations

$$\partial_t p - \langle \mathcal{L}_1 Pf\rangle = \epsilon\langle \mathcal{L}_1 Qf\rangle, \tag{4.15a}$$

$$\epsilon\partial_t Qf = \mathcal{L}_2 Qf + \mathcal{L}_1(Pf+\epsilon Qf) - \frac{1}{2\pi\Omega}\langle \mathcal{L}_1(Pf+\epsilon Qf)\rangle \tag{4.15b}$$

with operators $\mathcal{L}_1, \mathcal{L}_2$ defined in (4.2) and their projections $\langle \mathcal{L}_1 Pf\rangle, \langle \mathcal{L}_1 Qf\rangle$ given in (4.9b).

To zeroth order the system reduces to

$$\partial_t p - \langle \mathcal{L}_1 Pf\rangle = 0, \tag{4.16}$$

which gives the same result as obtained from the stochastic averaging theorem; compare (3.4a), (3.4b), (4.9a), and section 4.3.1. To first order in ϵ one obtains the system

$$\partial_t p - \langle \mathcal{L}_1 Pf\rangle = \epsilon\langle \mathcal{L}_1 Qf\rangle, \tag{4.17a}$$

$$-\mathcal{L}_2 Qf = \frac{1}{2\pi}\mathcal{L}_1\frac{p}{\Omega} - \frac{1}{2\pi\Omega}\langle \mathcal{L}_1 Pf\rangle \tag{4.17b}$$

as terms of order ϵ in (4.15b) are dropped since the term containing Qf in (4.15a) is of order ϵ. The computation of Qf from the second equation requires the inversion of the operator $\mathcal{L}_2$. Finally for second-order averaging we include terms up to order ϵ^2 in (4.15a) and up to order ϵ in (4.15b) for the same reason. We use the ansatz $Qf = U_1 + \epsilon U_2$. Then (4.15b) reads

(4.18)
$$\begin{aligned}\epsilon\partial_t(U_1+\epsilon U_2) &= \mathcal{L}_1 Pf + \mathcal{L}_2(U_1+\epsilon U_2) + \epsilon\mathcal{L}_1(U_1+\epsilon U_2) - \epsilon\langle \mathcal{L}_1 U_1 + \epsilon U_2\rangle \\ &= \mathcal{L}_1 Pf + \mathcal{L}_2 U_1 + \epsilon\mathcal{L}_2 U_2 + \epsilon\mathcal{L}_1 U_1 + \epsilon^2\mathcal{L}_1 U_2 - \epsilon\langle \mathcal{L}_1 U_1\rangle - \epsilon^2\langle \mathcal{L}_1 U_2\rangle .\end{aligned}$$

We drop ϵ^2 terms in (4.18) and gather terms of same order in ϵ. We hence have to solve the system

$$-\mathcal{L}_2 U_1 = \frac{1}{2\pi}\mathcal{L}_1\frac{p}{\Omega} - \frac{1}{2\pi\Omega}\langle \mathcal{L}_1 Pf\rangle , \tag{4.19a}$$

$$-\mathcal{L}_2 U_2 = \mathcal{L}_1 U_1 - \frac{1}{2\pi\Omega}\langle \mathcal{L}_1 U_1\rangle - \partial_t U_1 . \tag{4.19b}$$

Equation (4.19a) is identical to (4.17b) in first-order averaging, from which we obtain U_1. Then one has to compute $\mathcal{L}_1 U_1$. Finally, we have to determine $\partial_t U_1$ to zeroth order in ϵ.

In this way one obtains averaged equations where the coefficients are again computed by time averages over the unforced Hamiltonian motion of the original system. However, the appearing functions and their averages are in general not explicitly computable. We have to use numerical methods to determine the stochastic coefficients. In the next section, we present a simplified averaging procedure which will then be used together with a numerical approach to compare the stationary distribution of the full system (4.1) and the higher-order approximate energy process.

4.3. Further simplifications. To obtain an approximation which is easier to investigate we use an additional assumption to simplify the Q-equation. This assumption will yield accurate results as long as we are in a near-equilibrium situation.

Assumption 4.2 (proximity to equilibrium in p). *Approximate* $\partial_h \frac{p}{\Omega} = \partial_h Pf$ *by* $-\frac{p}{\Omega} = -Pf$ *in* (4.8b).

Remark 4.3. Using this assumption we will neglect several terms when compared to the rigorous second-order asymptotic analysis outlined in section 4.2. However, in a near-equilibrium situation they are expected to be small. These statements are supported by the numerical results in the following section.

With this assumption we have $\langle \mathcal{L}_1 Pf\rangle = 0$ and the Q-equation becomes

$$\epsilon\partial_t Qf - \mathcal{L}_2 Qf - \epsilon\mathcal{L}_1 Qf = \frac{1}{2\pi}\mathcal{L}_1\frac{p}{\Omega} - \epsilon\frac{1}{2\pi\Omega}\langle \mathcal{L}_1 Qf\rangle . \tag{4.20}$$

Note that, to leading order this yields $-\mathcal{L}_2 Qf$ is equal to a functional of p. Thus we can find a leading-order solution U_1 which depends on p and satisfies $\langle Qf\rangle = 0$. Using now the near-equilibrium assumption in (4.15a) yields $\partial_t p = 0$ to zeroth order. Moreover, this gives, to leading order, that $\partial_t Qf = 0$ since Q depends on p and its spatial derivatives. Thus, in the Q-equation, we can neglect $\epsilon\partial_t Qf$ as long as we do not proceed beyond a second-order analysis. Therefore, we consider

$$\partial_t p - \langle \mathcal{L}_1 Pf\rangle = \epsilon\langle \mathcal{L}_1 Qf\rangle , \tag{4.21a}$$

$$-\mathcal{L}_2 Qf - \epsilon\mathcal{L}_1 Qf = \frac{1}{2\pi}\mathcal{L}_1\frac{p}{\Omega} - \epsilon\frac{1}{2\pi\Omega}\langle \mathcal{L}_1 Qf\rangle . \tag{4.21b}$$

4.3.1. Zeroth order. According to the above remarks the coefficients to zeroth order equal the results of the stochastic averaging theorem and read

$$a(h) = \frac{A^2}{2}\overline{\sin^2\beta(z) - \cos^2\beta(z)}, \tag{4.22a}$$

$$\sigma^2(h) = A^2\overline{\cos^2\beta(z)}. \tag{4.22b}$$

No influence of friction is detected at zeroth order. The averaged equilibrium is the unforced equilibrium.

4.3.2. First order. We have to solve

$$\partial_t p - \langle \mathcal{L}_1 P f\rangle = \epsilon \langle \mathcal{L}_1 Q f\rangle\,, \tag{4.23a}$$

$$-\mathcal{L}_2 Q f = \frac{1}{2\pi}\mathcal{L}_1 \frac{p}{\Omega}. \tag{4.23b}$$

Terms of order ϵ in (4.21b) are dropped as the term containing Qf in (4.21a) is of order ϵ. We solve (4.23b) and insert this into (4.23a) to get averages. The right-hand side of (4.23b) is

$$\frac{1}{2\pi}\mathcal{L}_1\frac{p}{\Omega} = \frac{\kappa}{2\pi}\cos\phi H_r\frac{p}{\Omega} - \frac{\kappa}{2\pi}\frac{\sin\phi}{r}\cos\beta(z)\frac{p}{\Omega} + \frac{\kappa}{2\pi}\frac{\cos\phi}{r}\frac{p}{\Omega} \tag{4.24}$$

$$= \frac{\kappa}{2\pi\Omega}\left(\cos\phi\left(H_r + \frac{1}{r}\right) - \sin\phi\frac{\cos\beta(z)}{r}\right)p \tag{4.25}$$

$$= \frac{\kappa}{2\pi\Omega}\left(\cos\phi\cdot b(r) - \sin\phi\frac{\cos\beta(z)}{r}\right)p. \tag{4.26}$$

Using $Qf = U_1, c(r,z) = \frac{\sin\beta(z)}{r}$ this yields

$$H_r\partial_z U_1 - H_z\partial_r U_1 + c(r,z)\,\partial_\phi U_1 = \frac{\kappa}{2\pi\Omega}\left(\cos\phi\cdot b(r) - \sin\phi\frac{\cos\beta(z)}{r}\right)p. \tag{4.27}$$

We make the ansatz

$$U_1 = \kappa\mathrm{Re}\left\{\left[X(r,z)\frac{p}{2\pi\Omega}\right]e^{-i\phi}\right\} = \kappa\frac{p}{2\pi\Omega}(M\cos\phi + N\sin\phi) \tag{4.28}$$

with $X = M + iN$. This automatically guarantees $\overline{Qf} = 0$. Inserting this into (4.27), we obtain

$$H_r X_z - H_z X_r - icX = b(r) - i\frac{\cos\beta(z)}{r}, \tag{4.29a}$$

or

$$H_v M_v - H_x M_v + cN = b(r), \tag{4.30a}$$

$$H_v N_v - H_x N_v - cM = -\frac{\cos\beta(z)}{r}. \tag{4.30b}$$

Applying the method of characteristics gives

$$X = X(t) = C\,\mathrm{Hom}(t) + \mathrm{Inhom}(t), \tag{4.31a}$$

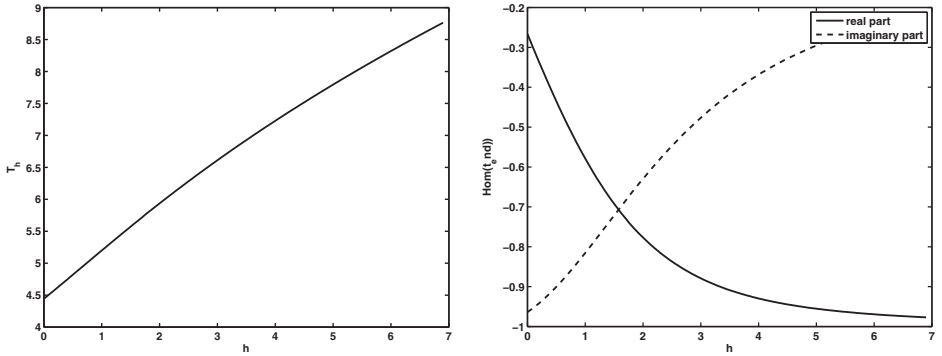

(a) Hamiltonian period length T_h (b) Homogenous solution $\mathrm{Hom}(T_h)$

FIG. 5. *Resonance investigation for the modified fiber models with $b(r)=r$. The given Hamiltonian motion in (r,z)-space is free of resonance when coupled with the secondary frequency* (2.14c)*, since we see numerically that $Hom(T_h)\neq 1$ for all h.*

where C is a constant and

$$\mathrm{Hom}(t)=\exp\left[i\int_0^t c(r_h(t'),z_h(t'))\,dt'\right], \tag{4.31b}$$

$$\mathrm{Inhom}(t)=\int_0^t\left(b(r_h)-i\frac{\cos\beta(z_h)}{r_h}\right)(t')\exp\left[i\int_{t'}^t c(r_h(t''),z_h(t''))\,dt''\right]dt'. \tag{4.31c}$$

Here, $(r_h(s),z_h(s))$ is the periodic solution of the unforced, deterministic Hamiltonian system. C is determined by the required periodicity of X, which implies that $X(0)=X(T_h)$ has to hold. This is possible as long as $\mathrm{Hom}(T_h)\neq 1$, i.e., there is no resonance. As the deterministic solutions are not explicit, we investigate resonance numerically. We illustrate T_h and $\mathrm{Hom}(T_h)$ for the case $b(r)=r$ in Figure 5, and conclude that the system is free of resonance. This is a priori not clear, since $c(r,z)$ is a function of the unforced, deterministic Hamiltonian evolution (r_h,z_h).

Remark 4.4. We note that this statement is not true in general. For example, for $b(r)=1$ we have for $h=0$ the period $T_h=2\pi$; see Remark 2.1. This gives $\mathrm{Hom}(T_h)=1$ and there is resonance.

Inserting the approximated solution for Qf into (4.8a), the resulting averaged equation to first order reads

$$\begin{aligned}
&\partial_t p+\frac{A^2}{2}\partial_h\left(\overline{\sin^2\beta(z)-\cos^2\beta(z)}p\right)-\frac{A^2}{2}\partial_h^2\left(\overline{\cos^2\beta(z)}p\right)\\
&\quad=-\epsilon\kappa\partial_h\langle H_r\cos\phi U_1\rangle+\epsilon\kappa\partial_h\left\langle\frac{1}{r}\cos\beta(z)\sin\phi U_1\right\rangle\\
&\quad\quad-\epsilon\frac{A^2}{2}\partial_h\left\langle(\sin^2\beta(z)-\cos^2\beta(z))U_1\right\rangle+\epsilon\frac{A^2}{2}\partial_h^2\left\langle\cos^2\beta(z)U_1\right\rangle\\
&\quad=\frac{\epsilon\kappa^2}{2}\partial_h\left(\left(-\overline{H_rM}+\overline{\frac{\cos\beta(z)}{r}N}\right)p\right).
\end{aligned} \tag{4.32}$$

The corresponding averaged stochastic coefficients are

$$a(h) = \frac{A^2}{2}\left(\overline{\sin^2\beta(z) - \cos^2\beta(z)}\right) + \frac{\epsilon\kappa^2}{2}\left(\overline{H_r M} - \overline{\frac{\cos\beta(z)}{r}N}\right), \tag{4.33}$$

$$\sigma^2(h) = A^2\overline{\cos^2\beta(z)}. \tag{4.34}$$

Evaluating the first-order term in $a(h)$ numerically yields a vanishing first-order contribution. Thus, the contribution of the moving belt to the first-order averages is again equal to zero as in the zeroth-order case. There is still no influence of the belt motion on the averaged equations.

4.3.3. Second order. In order to capture the influence of the forcing on the limit equations we include terms up to order ϵ^2 in system (4.21). We use the ansatz $Qf = U_1 + \epsilon U_2$. Then, as again the term containing Qf in (4.21a) is of order ϵ, we drop terms of order ϵ^2 in (4.21b) and gather terms of same order in ϵ. We hence have to solve the system

$$-\mathcal{L}_2 U_1 = \frac{1}{2\pi}\mathcal{L}_1\frac{p}{\Omega}, \tag{4.35a}$$

$$\mathcal{L}_2 U_2 = -\mathcal{L}_1 U_1 - \langle \mathcal{L}_1 U_1\rangle. \tag{4.35b}$$

Equation (4.35a) has already been solved above and U_1 is known. We first have to compute $\mathcal{L}_1 U_1$:

$$\begin{aligned}\mathcal{L}_1 U_1 = {} & -\kappa\partial_r(\cos\phi U_1) - \kappa\partial_z\left(\frac{\sin\phi}{r}U_1\right) + \partial_\phi\left(\kappa\sin\phi\frac{1}{r}U_1\right)\\ & - \frac{A^2}{2}\partial_z(\cos\beta U_1) + \frac{A^2}{2}\partial_z^2 U_1.\end{aligned} \tag{4.36}$$

This is equal to

$$\begin{aligned}\mathcal{L}_1 U_1 = {} & -\kappa\partial_r\left(\cos\phi\frac{\kappa p}{2\pi\Omega}(M\cos\phi + N\sin\phi)\right) - \kappa\partial_z\left(\frac{\sin\phi}{r}\frac{\kappa p}{2\pi\Omega}(M\cos\phi + N\sin\phi)\right)\\ & + \partial_\phi\left(\kappa\sin\phi\frac{1}{r}\frac{\kappa p}{2\pi\Omega}(M\cos\phi + N\sin\phi)\right)\\ & - \frac{A^2}{2}\partial_z\left(\cos\beta\kappa\frac{p}{2\pi\Omega}(M\cos\phi + N\sin\phi)\right) + \frac{A^2}{2}\partial_z^2\kappa\frac{p}{2\pi\Omega}(M\cos\phi + N\sin\phi).\end{aligned}$$

One can compute that this expression is equal to

$$\begin{aligned}\mathcal{L}_1 U_1 = {} & \frac{\kappa^2 p}{2\pi\Omega}\left(\cos^2\phi\cdot G(M) + \sin^2\phi\cdot H(M,N) + \cos\phi\sin\phi\cdot J(M,N)\right)\\ & + \frac{A^2\kappa p}{4\pi\Omega}\left(\cos\phi\cdot F(M) + \sin\phi\cdot F(N)\right),\end{aligned} \tag{4.37}$$

where G, H, J, F are defined as

$$G(M) = Mb(r) - \partial_r M, \tag{4.38a}$$

$$H(M,N) = -\frac{N\cos\beta}{r} - \frac{1}{r}\partial_z N - \frac{M}{r}, \tag{4.38b}$$

$$J(M,N) = Nb(r) - \partial_r N - \frac{M\cos\beta}{r} + \frac{N}{r} - \frac{1}{r}\partial_z M, \tag{4.38c}$$

$$F(M) = \cos\beta\partial_z M + \partial_z^2 M. \tag{4.38d}$$

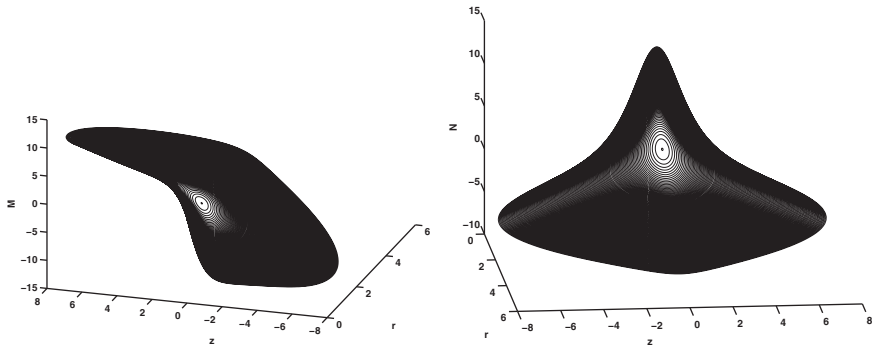

(a) M(r,z) (b) N(r,z)

FIG. 6. *The surfaces M and N in (r,z)-space for the modified fiber model. Due to the nonlinearity of the model, both functions are much harder to numerically differentiate than the oscillator equations in* [5] *and sufficient accuracy is obtained using the strategy introduced in section* 5.

The derivatives of M,N are computed as explained in section 5. Sufficient approximation quality is only achieved using the strategy explained there. The nonpolynomic surfaces M and N in (r,z)-space are illustrated in Figure 6. To solve (4.35b), we split the problem into two equations

$$\mathcal{L}_2 U_2^\kappa = -(\mathcal{L}_1 U_1)^\kappa + \langle \mathcal{L}_1 U_1 \rangle \,, \tag{4.39a}$$

$$\mathcal{L}_2 U_2^A = -(\mathcal{L}_1 U_1)^A \,, \tag{4.39b}$$

where the right-hand side in (4.39a) includes the parts of order κ^2 in (4.37) and the right-hand side of (4.39b) includes those of order κA^2. The ansatz for solving equation (4.39b) is as in the first-order case

$$U_2^A = \frac{A^2\kappa}{2}(M^A\cos\phi + N^A\sin\phi)\frac{p}{2\pi\Omega}\,. \tag{4.40}$$

This yields

$$\sin\beta H_r M_\beta^A + \cos\beta M_r^A + \frac{\sin\beta}{r}N^A = F(M)\,, \tag{4.41a}$$

$$\sin\beta H_r N_\beta^A + \cos\beta N_r^A - \frac{\sin\beta}{r}M^A = F(N)\,. \tag{4.41b}$$

Applying the method of characteristics gives the system

$$\dot\beta = \sin\beta H_r \,, \tag{4.42a}$$

$$\dot r = \cos\beta \,, \tag{4.42b}$$

$$\dot X^A = i\frac{\sin\beta}{r}X + F(M) + iF(N) \tag{4.42c}$$

with $X^A = M^A + iN^A$. The resulting second-order averages to be added to (4.32) are

$$-\frac{A^2\kappa^2\epsilon^2}{4}\partial_h\left(\overline{H_r M^A - \frac{\cos\beta}{r}N^A p}\right). \tag{4.43}$$

Here, an additional factor $\kappa\epsilon$ arrives from the original equation for Pf. Finally we have to solve (4.39a). The ansatz for U_2^κ is

$$U_2^\kappa = \kappa^2 \frac{p}{2\pi\Omega}\left(M^\kappa\left(\cos^2\phi - \frac{1}{2}\right) + N^\kappa \cos\phi\sin\phi + R^\kappa\right). \tag{4.44}$$

This gives

$$\dot\beta = \sin\beta\, H_r, \tag{4.45a}$$
$$\dot r = \cos\beta, \tag{4.45b}$$
$$\dot M^\kappa + \frac{\sin\beta}{r} 2N^\kappa = G(M) - H(M,N), \tag{4.45c}$$
$$\dot N^\kappa - \frac{\sin\beta}{r} 2M^\kappa = J(N,M), \tag{4.45d}$$
$$\dot R^\kappa = \frac{1}{2}\left(G(M) + H(M,N) - \langle G(M) + H(M,N)\rangle\right), \tag{4.45e}$$

or

$$\dot X^\kappa = i\frac{\sin\beta}{r} X + G(M) - H(M,N) + iJ(N,M), \tag{4.46a}$$
$$\dot R^\kappa = \frac{1}{2}\left(G(M) + H(M,N) - \langle G(M) + H(M,N)\rangle\right) \tag{4.46b}$$

with $X^\kappa = M^\kappa + iN^\kappa$.

As before, we require periodicity of X^κ. Moreover, in this case, $\overline{U_2^\kappa}$ has to be equal to 0 to get $\overline{Qf} = 0$. This is true, if $\overline{R^\kappa} = 0$, which is a condition to fix R^κ. This yields

$$R^\kappa = \int_0^t \frac{1}{2}(G(M) + H(M,N) - \langle G(M) + H(M,N)\rangle)\,\mathrm{d}t'.$$

We obtain the following additional second-order averages

$$\begin{aligned} &-\epsilon\frac{A^2}{2}\partial_h\left\langle(\sin^2\beta(z) - \cos^2\beta(z))U_2^k\right\rangle + \epsilon\frac{A^2}{2}\partial_h^2\left\langle\cos^2\beta(z)U_2^k\right\rangle \\ &\quad = -\frac{A^2k^2\epsilon^2}{2}\partial_h\left(\overline{(\sin^2\beta - \cos^2\beta)R^\kappa}p\right) \\ &\qquad + \frac{A^2k^2\epsilon^2}{2}\partial_h^2\left(\overline{\cos^2\beta R^\kappa}p\right). \end{aligned} \tag{4.47}$$

Altogether, the second-order coefficients are

$$\begin{aligned} a(h) = {} & \frac{A^2}{2}\left(\overline{\sin^2\beta(z) - \cos^2\beta(z)}\right) + \frac{\epsilon\kappa^2}{2}\left(\overline{H_r M} - \overline{\frac{\cos\beta(z)}{r}N}\right) \\ & + \frac{A^2\kappa^2\epsilon^2}{4}\overline{H_r M^A - \frac{\cos\beta}{r}N^A} + \frac{A^2\kappa^2\epsilon^2}{2}\overline{(\sin^2\beta - \cos^2\beta)R^\kappa}, \end{aligned} \tag{4.48a}$$
$$\sigma^2(h) = A^2\overline{\cos^2\beta(z)} + A^2\kappa^2\epsilon^2\overline{\cos^2\beta R^\kappa}, \tag{4.48b}$$

and the corresponding Fokker–Planck equation again reads

$$\partial_t p + \partial_h(a(h)p) = \frac{1}{2}\partial_h^2(\sigma^2(h)p). \tag{4.49}$$

Remark 4.5. We note that compared to the outline of the asymptotic analysis from section 4.2 where the near equilibrium assumption has not been used, there are several terms approximated by zero. These terms do not cancel out in a rigorous asymptotic analysis. However, in a near-equilibrium situation they are expected to be small. These statements are supported by the numerical results in the next section.

We have obtained averaged coefficients of higher order, which are again computed by time averages over the unforced Hamiltonian motion of the original system. However, the appearing functions and their averages are in general not explicitly computable. We have to use numerical methods to determine the stochastic coefficients. It is important to point out that the influence of the periodic forcing terms induced by the belt motion on the energy process is only visible in the second-order averaged coefficients (4.48). A similar effect has been observed in [5] for standard linear and nonlinear oscillator systems. At least in the linear case, all computations were explicit, as were the resulting averaged coefficients. In the present case, all computations have to be performed using numerical methods due to the strongly nonlinear terms in the model. The computation of $\mathcal{L}_1 U_1$ is particularly critical, as partial derivatives of numerical functions given on discretized Hamiltonian spheres have to be computed at high accuracy. In the next section, we present our numerical approach together with numerical results comparing the stationary distribution of the full system and of the higher-order approximate energy process with the second-order coefficients (4.48).

5. Numerical results. In this section the numerical methodology to determine the numerical averages for the limiting coefficients is explained in detail. For the stochastic averaging theorem, finding drift and diffusion coefficients is reduced to averaging along Hamiltonian spheres

$$\bar{f}(h) := \frac{1}{T_h}\int_0^{T_h} f(r(s),z(s))\mathrm{d}s, \tag{5.1}$$

which can be treated easily with standard numerical methods. The evaluation of averages is also a numerical component of the presented higher-order ansatz. Additionally, further integrals along spheres have to be evaluated involving the functions M,N for first-order, and M^A,N^A,R^κ for second-order averaging. In our code, we use a standard adaptive fourth-order Runge–Kutta method available in MATLAB (see [8]) to solve the deterministic Hamiltonian system for a fixed number of energy values, which is slightly modified to detect the period length T_h which is a priori unknown. Using a nonsymplectic time integration is feasible as only one orbit of the periodic motion on the time discretized time grid $[0,T_h]$ is required. Numerical integration along the adaptive time grid is done with a standard second-order quadrature formula.

A more challenging problem is the numerical spatial differentiation of M,N in the second-order procedure. Recall, that M_r,M_z,M_{zz},N_r,N_z form the right-hand side of (4.38). We have to compute partial derivatives using only function values that are given on the adaptively discretized Hamiltonian spheres. Instead of a regular grid, data are only available on point clouds. To overcome this difficulty, we use a

moving least squares approximation (see [16]), which is similar to the differentiation techniques used in meshfree methods (see, e.g., [21]). The basic idea is the following: Fix any point $p=(x,y)\in\mathbb{R}^2$ and let B_p be a set of neighboring data points. By a Taylor expansion, for any $p_i=(x_i,y_i)\in B_p$,

$$f(p_i)=f(p)+\nabla f(p)\cdot\begin{pmatrix}\Delta x_i\\ \Delta y_i\end{pmatrix}+\frac{1}{2}\left(\Delta x_i,\,\Delta y_i\right)\cdot\text{Hess }f(p)\cdot\begin{pmatrix}\Delta x_i\\ \Delta y_i\end{pmatrix}+e_i, \tag{5.2}$$

where $\Delta x=x_i-x,\Delta y=y_i-y$, and e_i denotes the error term. With a restriction to two dimensions there are five unknowns

$$(a_1,\dots,a_5)^T=(\partial_x f(p),\,\partial_y f(p),\,\partial_{x^2} f(p),\,\partial_x\partial_y f(p),\,\partial_{y^2} f(p))^T.$$

Writing (5.2) for all N_p points $p_i\in B_p$, we get the linear system

$$e=Ma-b \tag{5.3}$$

with $e=(e_1,\dots,e_{N_p})^T$, $b=(f(p_1)-f(p),\dots,f(p_{N_p})-f(p))^T$, and

$$M=\begin{pmatrix}\Delta x_1 & \Delta y_1 & \frac{1}{2}\Delta x_1^2 & \Delta x_1\Delta y_1 & \frac{1}{2}\Delta y_1^2\\ \vdots & \vdots & \vdots & \vdots & \vdots\\ \Delta x_{N_p} & \Delta y_{N_p} & \frac{1}{2}\Delta x_{N_p}^2 & \Delta x_{N_p}\Delta y_{N_p} & \frac{1}{2}\Delta y_{N_p}^2\end{pmatrix}. \tag{5.4}$$

The approximation vector a is now obtained by a weighted least squares minimization of e. Denote

$$J_p(a):=\sum_{i=1}^{N_p} w_i e_i^2=(Ma-b)^T W(Ma-b) \tag{5.5}$$

with weights w_i and $W=\text{diag}(w_1,\dots,w_{N_p})$. Then the minimizing condition $\nabla_a J_p=0$ leads to the normal equation

$$(M^TWM)a=M^TWb, \tag{5.6}$$

which is solved with standard methods. The weights are chosen to decay exponentially with relative distance such that

$$w_i(p,p_i)=\exp(-\gamma\|p_i-p\|_2^2). \tag{5.7}$$

This procedure has to be repeated for all data points of the discretized Hamiltonian spheres.

In contrast to some meshfree methods, the data points considered in this problem are fixed by the adaptive ODE solver. The condition of (5.6) and the approximation quality of the derivatives highly depends on the choice of the neighborhood B_p. Points have to be filtered to avoid an ill-conditioned linear system which, e.g., happens if no spatial information towards one direction is selected. We discuss three algorithm for neighborhood selection and compare their performance. Let $p=(x,y)$ a fixed point and $r_i:=\|p_i-p\|_2$ the relative distance to all other points. In order to determine B_p, the three strategies are as follows.

- Plain disc (PD). Set a maximal distance R^* and $B_p:=\{p_i:r_i\le R^*\}$. A typical choice for the given problems is $R^*=3$.
- Angular division (AD). Set a minimal distance r^* and a maximal distance R^* and consider only points with $r^*\le r_i\le R^*$. Compute the angle α_i of the distance vector p_i-p for every point and group neighbor points into six equally sized angular segments of $[0,2\pi)$. In every segment, points are sorted

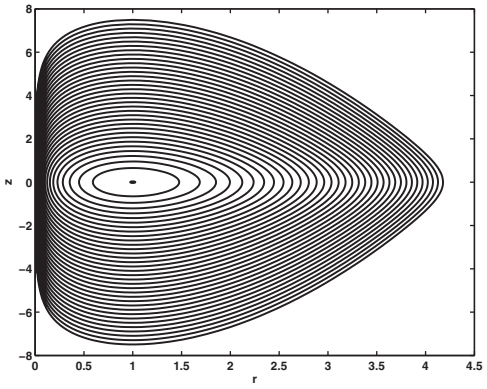

FIG. 7. *The unforced Hamiltonian spheres for the fiber model* (2.14). *In order to apply the method of higher-order stochastic averaging, functions with values defined on discretized spheres have to be spatially differentiated twice.*

ascending with r_i and a maximum of k points is selected for B_p. Typical choices for the given problems are $r^* = 10^{-4}$, $R^* = 3$, $k \in [5,40]$.

- Adaptive angular division (AAD). Set a minimal distance r^* and consider only points with $r^* \le r_i$. Compute the angle α_i of the distance vector $p_i - p$ for every point and group neighbor points into six equally sized angular segments of $[0,2\pi)$. Now, iterate an increasing maximal distance R^* and consider points with $r_i \le R^*$ until the following conditions are fulfilled:
  - at least K neighbors are selected ($|B_p| \ge K$);
  - at least 3 segments contain points;
  - the mean relative distance exceeds a minimum threshold

$$\frac{1}{|B_p|} \sum_{p_i \in B_p} r_i \ge \delta . \tag{5.8}$$

Typical choices for the given problems are $r^* = 10^{-4}$, $R^* = 3$, $K = 40$, $\delta = 0.05$. We illustrate the performance of the proposed strategies with the two test functions

$$f_1(r,z) := \sin(r)\sin(z)\,,\; f_2(r,z) = e^{-(r^2+z^2)}\,, \tag{5.9}$$

given on discretized, unforced Hamiltonian spheres of the fiber model (2.14). The spheres of the fiber equation are only available from a numerical integration of the ODE system. We fix the set of energy levels to $h \in \{0, 0.05, 0.1, \ldots, 6.9\}$ and show some of the resulting spheres of constant energy in phase space in Figure 7. In order to measure the total error $\|\overline{\partial_x f} - \partial_x f\|$ between the numerical approximation $\overline{\partial_x f}$ and any explicitly computable partial derivatives of $\partial_x f$ on the active domain in (r,z)-space, we define the error functional

$$E(\partial_x f, \overline{\partial_x f}) := \sum_{k=1}^{N} \beta_k(p_k) |\partial_x f(p_k) - \overline{\partial_x f}(p_k)|\,, \tag{5.10}$$

with point-dependent weights

$$\beta_k(p_k) := \min_{l \ne k} \|p_k - p_l\|_2 \tag{5.11}$$

TABLE 1

Total approximation error E (defined in (5.10)) for partial derivatives of two test functions (see (5.9)) and different neighborhood point set methods: The AAD selection strategy produces significantly better results than PD and AD. The precision obtained through AAD has a decisive impact on the accuracy of higher-order stochastic averages, where derivatives must be computed accurately on irregular grids.

E		f_1			f_2	
	PD	AD	AAD	PD	AD	AAD
∂_r	4.594e-2	9.499e-3	2.269e-3	9.552e-3	1.767e-3	4.382e-4
∂_z	4.588e-2	1.168e-2	2.751e-3	1.255e-2	1.523e-3	4.219e-4
∂_r^2	6.513e-2	1.826e-2	4.108e-3	3.036e-2	6.001e-3	1.041e-3
∂_z^2	6.391e-2	1.223e-2	4.394e-3	2.025e-2	3.795e-3	9.853e-4

chosen as the distance to the closest neighboring point in order to normalize the error functional with respect to the varying point density in the discretization of the Hamiltonian spheres. Here, N is the total number of discretization points for the set of spheres. The resulting approximation errors of method (5.2), (5.6) are summarized in Table 1. It can be seen that AAD significantly outperforms PD and AD in terms of approximation error and thus has been used for all computations. We note, that the approximation error per sphere is significantly smaller than the total error E as the number of spheres in the example is $\mathcal{O}(10^2)$. As the higher-order averaging procedure additionally involves averages along the spheres, the approximation error of AAD is small enough to reliably compute the small deviations shown in the results below.

Remark 5.1. We would like to stress that the necessity of accurate derivative approximations increases with more involved unforced spheres and less smooth functions M,N to be differentiated. The derivation of AAD therefore marks a key improvement in using higher-order stochastic averaging for highly nonlinear problems such as model (2.14). For other problems, finding suitable parameter values is a first step in the computation of higher-order stochastic averages.

We now return to the numerical results of our averaging procedure. The resulting higher-order stochastic averaging coefficients are illustrated in Figure 8 for the setting $\kappa=0.2, A=\sqrt{\kappa}, \epsilon=1$. The second-order terms of (4.48) are plotted for $\kappa=0.1, A=\sqrt{\kappa}, \epsilon=1$, and $h\in[0,1.5]$ in Figure 9.

The stationary energy distribution of the averaged equation with coefficients (4.48) is compared to a Monte Carlo simulation of system (2.14) in Figure 10 for the parameter set $\kappa\in\{0.1,0.2\}, A=\sqrt{\kappa}$. Additionally, the difference to the unforced stationary solution ($\kappa=0$) is plotted for both the higher-order averaging equilibrium and the Monte Carlo simulation in Figure 11. Monte Carlo simulations for the full system are computed with $M=1000000$ runs on time grid $T=[0,500]$, $\Delta t=0.001$, and initial condition $f_0(x,v,\phi)\sim\delta_{rz}(r=1,z=0)\cdot\mathcal{U}_\phi([0,2\pi])$. The asymptotic stationary distribution of higher-order averaging is computed based on the higher-order coefficients via the solution formula of (4.49) as

$$p_s(h)=C\exp\left(\int_0^h \frac{2a(h')-\partial_h\sigma^2(h')}{\sigma^2(h')}dh'\right). \tag{5.12}$$

The results show a very good agreement between the fully simulated disturbed equilibrium under deterministic friction and the asymptotic higher-order averages derived in this work. Due to the nonlinearity of the model and the less smooth surfaces M,N, the approximation only holds for smaller values of κ as in [5]. Higher-

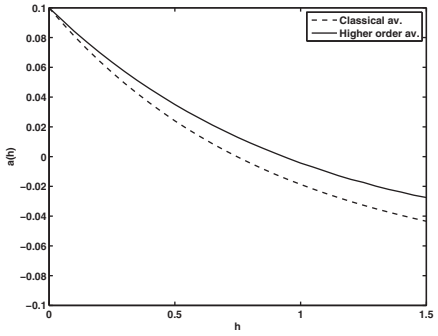

(a) drift $a(h)$

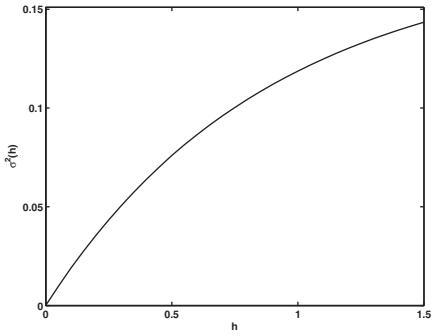

(b) diffusion $\sigma^2(h)$ for zeroth-order averaging

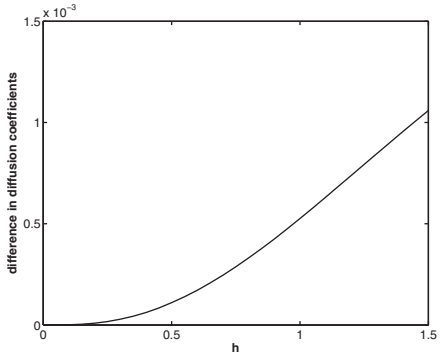

(c) $\sigma^2(h)$: difference of higher-order and zeroth-order diffusion ((4.48b) − (4.22b))

FIG. 8. *Resulting higher-order coefficients for the modified fiber model* (2.14) ($\kappa = 0.2, A = \sqrt{\kappa}, \epsilon = 1$).

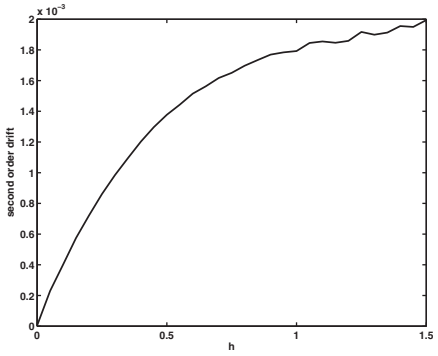

(a) second-order component of $a(h)$

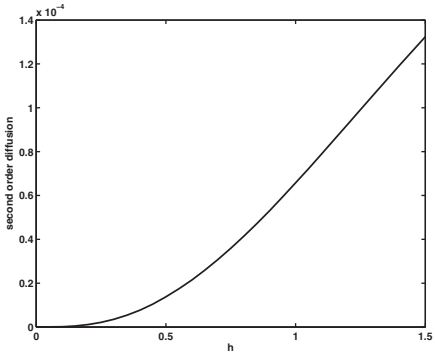

(b) second-order component of $\sigma^2(h)$

FIG. 9. *Second-order terms of the averaged coefficients* (4.48) *for low energy values and* $\kappa = 0.1, A = \sqrt{\kappa}, \epsilon = 1$.

order stochastic averages prove to be correct for small scale ϵ and an understanding of the influence of the periodic forcing upon the energy process is gained by studying its effect on the averaged coefficients in second order.

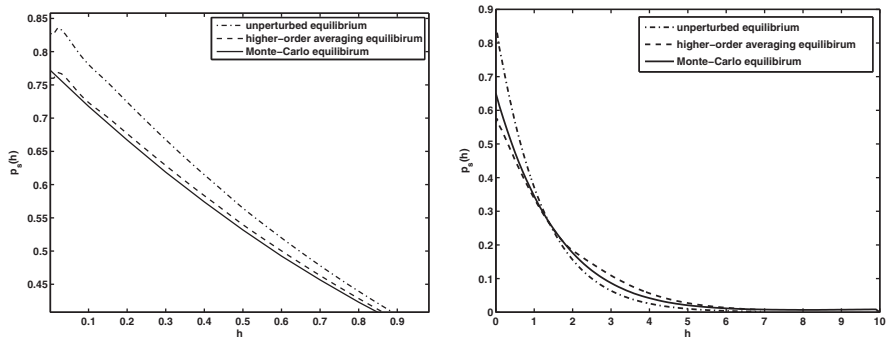

(a) $\kappa = 0.1$ (b) $\kappa = 0.2$

FIG. 10. *Energy equilibria resulting from higher-order stochastic averaging compared to a Monte Carlo simulation and the unforced equilibrium* ($\kappa = 0$) *for* $\kappa \in \{0.1, 0.2\}, A = \sqrt{\kappa}, \epsilon = 1$ *for the modified fiber model* (2.14). *Unforced, higher-order averaging* (4.48) *and Monte Carlo simulation of* (2.14) *are shown.*

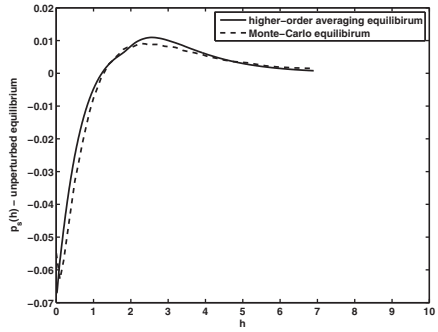

FIG. 11. *Energy equilibria resulting from higher-order stochastic averaging: difference to unforced equilibrium* $\kappa = 0$ *for the higher-order averaging equilibrium* $(-)$ *and the Monte Carlo simulation* $(--)$ *for the case* $\kappa = 0.1, A = \sqrt{A}, \epsilon = 1$. *The agreement confirms the validity of the higher-order averaging method.*

6. Conclusions. In this paper, we have investigated a modified model for a fiber lay-down process based on a Fokker–Planck equation in the limit of small noise and small turbulence. The model discussed reassembles a production process, where the rotational direction of the fiber induced by the spinning nozzles has strong influence on the lay-down process, which wiggles stochastically but does not randomly change its rotational direction. We have illustrated that the unperturbed stationary energy distribution of this model is stabilized by a balance of force and noise terms in the coordinates (r, z), whereas the corresponding equilibrium in the original model is obtained as a homogenization over a periodic torus. Thanks to the stability of the unperturbed equilibrium, we were able to apply the higher-order averaging procedure developed in [5] to this model. We have used a similar splitting ansatz to obtain an equation for the energy dependent density Pf and its remainder Qf. With an approximate solution of Qf, higher-order approximations of Pf have been computed. As in the simpler cases, we have been able to observe that higher-order approximations are necessary to assess the influence of the moving belt on the limiting energy distribution. More precisely, the contribution is only observed for a second-order approximation

since all first-order approximation terms are zero. The computation of second-order averaged coefficients requires the differentiation of functions in phase space defined on deterministic Hamiltonian spheres of constant energy. Only when these derivatives are computed accurately do the resulting coefficients become a valid approximation. To do so, an efficient neighborhood selection algorithm for the irregular point cloud has been found.

Comparing this to Monte Carlo simulations, the second-order approximation shows a very accurate match to the full systems dynamics for the examples that have been investigated, as long as the belt motion is not too fast.

We hence demonstrated that the method introduced in [5] is applicable to highly nonlinear Hamiltonian systems, such as the new modified fiber model. It produces correct approximations of the deviations of stationary states for small perturbations, under the condition that the arising numerical problems, whose difficulty scales with the nonlinearity of the system, can be solved accurately enough.

REFERENCES

[1] S. Albeverio and A. Klar, *Longtime behaviour of nonlinear stochastic oscillators*, J. Math. Phys., 35 (1994), pp. 4005–4027.

[2] S. Albeverio and A. Klar, *Longtime behaviour of stochastic Hamiltonian systems*, Potential Anal., 12 (2000), pp. 281–297.

[3] V.I. Arnold, *Mathematical Methods of Classical Mechanics*, Springer, New York, 1978.

[4] L.L. Bonilla, T. Götz, A. Klar, N. Marheineke, and R. Wegener, *Hydrodynamic limit of a Fokker–Planck equation describing fiber lay–down processes*, SIAM J. Appl. Math., 68 (2007), pp. 648–665.

[5] L.L. Bonilla, A. Klar, and S. Martin, *Higher order averaging of linear Fokker–Planck equations with periodic forcing*, SIAM J. Appl. Math., 72 (2012), pp. 1315–1342.

[6] L.L. Bonilla and S.W. Teitsworth, *Nonlinear Wave Methods for Charge Transport*, Wiley-VCH, Weinheim, Germany, 2010.

[7] J. Dolbeault, A. Klar, C. Mouhot, and C. Schmeiser, *Hypocoercivity and a Fokker-Planck equation for fiber lay-down*, Appl. Math. Res. Express, 2013 (2013), pp. 165–175.

[8] J.R. Dormand and P.J. Prince, *A family of embedded Runge-Kutta formulae*, J. Comput. Appl. Math., 6 (1980), pp. 9–26.

[9] T. Götz, A. Klar, N. Marheineke, and R. Wegener, *A stochastic model and associated Fokker-Planck equation for the fiber lay-down process in nonwoven production processes*, SIAM J. Appl. Math., 67 (2007), pp. 1704–1717.

[10] R.Z. Khasminskii, *The behaviour of a conservative system under the action of slight friction and slight random forces*, Prikl. Mat. Mekh., 28 (1964), pp. 931–935.

[11] R.Z. Khasminskii and G. Yin, *On averaging principles: An asymptotic expansion approach*, SIAM J. Math. Anal., 35 (2004), pp. 1534–1560.

[12] R.Z. Khasminskii and G. Yin, *Asymptotic series for singularly perturbed Kolmogorov–Fokker–Planck equations*, SIAM J. Appl. Math., 56 (1996), pp. 1766–1793.

[13] A. Klar, N. Marheineke, and R. Wegener, *Hierarchy of mathematical models for production processes of technical textiles*, ZAMM Z. Angew. Math. Mech., 89 (2009), pp. 941–961.

[14] A. Klar, J. Maringer, and R. Wegener, *A 3d model for fiber lay-down in nonwoven production processes*, Math. Methods Appl. Sci., 22 (2012), 1250020.

[15] A. Klar, J. Maringer, and R. Wegener, *A smooth 3d model for fiber lay-down in nonwoven production processes*, Kinetic Relat. Models, 5 (2012), pp. 97–112.

[16] D. Levin, *The approximation power of moving least squares*, Math. Comp., 67 (1998), pp. 1517–1531.

[17] L. Mahadevan and J.B. Keller, *Coiling of flexible ropes*, R. Soc. Lond. Proc. Ser. A Math. Phys. Eng. Sci., 452 (1996), pp. 1679–1694.

[18] N. Marheineke and R. Wegener, *Fiber dynamics in turbulent flows: General modeling framework*, SIAM J. Appl. Math., 66 (2006), pp. 1703–1726.

[19] G. Papanicolaou, D. Stroock, and S. Varadhan, *Martingale approach to some limit theorems*, in Statistical Mechanics and Dynamical Systems, D. Ruelle, ed., Duke Univ. Math. Ser. III, Durham, NC, 1977, paper 6.

[20] H. Risken, *The Fokker-Planck Equation*, Springer Berlin, 1996.
[21] S. Tiwari and J. Kuhnert, *Finite pointset method based on the projection method for simulations of the incompressible Navier-Stokes equations*, in Meshfree Methods for Partial Differential Equations, Lect. Notes Comput. Sci. Eng. 26, M. Griebel and M. A. Schweitzer, eds., Springer, Berlin, 2003, pp. 373–387.
[22] R. Zwanzig, *Nonequilibrium Statistical Mechanics*, Oxford University Press, New York, 2001.